View metadata, citation and similar papers at core.ac.uk
brought to you by CORE
provided by Infoscience - École polytechnique fédérale de Lausanne

Japanese Journal of Applied Physics **50** (2011) 111002
REGULAR PAPER
DOI: 10.1143/JJAP.50.111002

Implementation of Spatio-Time-Resolved Cathodoluminescence Spectroscopy for Studying Local Carrier Dynamics in a Low Dislocation Density *m*-Plane $In_{0.05}Ga_{0.95}N$ Epilayer Grown on a Freestanding GaN Substrate

Munehito Kagaya, Pierre Corfdir[1], Jean-Daniel Ganière[1], Benoît Deveaud-Plédran[1], Nicolas Grandjean[1], and Shigefusa F. Chichibu*

CANTech, Institute of Multidisciplinary Research for Advanced Materials, Tohoku University, Sendai 980-8577, Japan
[1]*Institute of Condensed Matter Physics, Ecole Polytechnique Federale de Lausanne (EPFL), 1015 Lausanne, Switzerland*

Received May 27, 2011; revised August 11, 2011; accepted September 11, 2011; published online October 27, 2011

Spatio-time-resolved cathodoluminescence (STRCL) spectroscopy is implemented to assess the local carrier dynamics in a 70-nm-thick, very low threading dislocation (TD) density, pseudomorphic *m*-plane $In_{0.05}Ga_{0.95}N$ epilayer grown on a freestanding GaN substrate by metalorganic vapor phase epitaxy. Although TDs or stacking faults are absent, sub-micrometer-wide zonary patterns parallel to the *c*-axis and 2-μm-long-axis figure-of-8 patterns parallel to the *a*-axis are clearly visualized in the monochromatic cathodoluminescence intensity images. Because the STRCL measurement reveals very little spatial variation of low-temperature radiative lifetime, the considerable peak energy variation is interpreted to originate from nonidentical In-incorporation efficiency for the growing surfaces exhibiting various miscut angles. The figure-of-8 patterns are ascribed to originate from the anisotropic, severe *m*-plane tilt mosaic along the *a*-axis of the GaN substrate, and the zonary patterns may originate from the *m*-plane tilt mosaic along the *c*-axis. © 2011 The Japan Society of Applied Physics

1. Introduction

Wurtzite group-III nitride semiconductors grown in nonpolar and semipolar orientations[1)] are a promising candidate for realizing high performance ultimate optoelectronic devices. This is because the quantum wells (QWs) fabricated on off-polar planes suffer from less-pronounced unwanted quantum-confined Stark effects (QCSEs) caused by the immobile interfacial charges induced by the polarization discontinuity along the *c*-axis.[2–4)] To date, InGaN/GaN high brightness light emitting diodes[5)] and laser diodes[6–9)] have been demonstrated using low threading dislocation (TD) density, low basal-plane stacking fault (BSF) density *m*-[5–7)] and (20$\bar{2}$1)-plane[8,9)] freestanding GaN substrates (FS-GaN) that were sliced from a thick *c*-plane FS-GaN boule grown by halide vapor phase epitaxy.[10)]

One of the drawbacks of nonpolar and semipolar growths is that BSFs propagate throughout the epilayer once they are formed. In addition, unintentional miscut of the substrate surface gives rise to the evolution of inclined planes, resulting in undulated surface morphology of GaN.[11)] Also, because the state-of-the-art *m*-plane FS-GaN[10)] is usually sliced from certainly bowed *c*-plane FS-GaN, the tilt and twist mosaics of the initial *c*-plane substrate are transferred to in-plane twist plus *m*-plane tilt mosaic along the *c*-axis and anisotropic greater *m*-plane tilt mosaic along the *a*-axis, respectively, as shown in Figs. 1(a) and 1(b). Accordingly, there remain concerns if such structural imperfections would cause inhomogeneous incorporation of In during the InGaN growths,[12–14)] because the In-incorporation efficiency differs depending on the crystallographic orientation of the growth front. As a matter of fact, the full-width at half-maximum (FWHM) values for the near-band-edge (NBE) photoluminescence (PL) peak of the *m*-plane $In_xGa_{1-x}N$ epilayers[5,15)] grown by metalorganic vapor phase epitaxy (MOVPE) on FS-GaN were larger than those for *c*-plane $In_xGa_{1-x}N$ epilayers[16)] of the same InN mole fractions (x).

In order to assess local carrier dynamics in a semiconductor, Merano *et al.*[17)] have recently developed a pico-

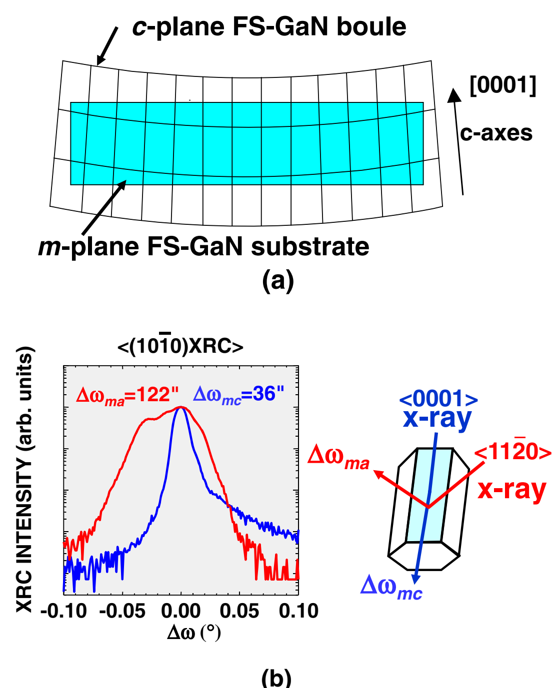

Fig. 1. (Color online) (a) Schematic cross-sectional representation of a *c*-plane FS-GaN boule detached from a sapphire substrate grown by halide vapor phase epitaxy. The shaded rectangle represents an *m*-plane FS-GaN substrate sliced from the *c*-plane FS-GaN. (b) XRCs for the (10$\bar{1}$0) diffraction of the *m*-plane FS-GaN substrate. $\Delta\omega_{mc}$ and $\Delta\omega_{ma}$ represent the FWHM values for the (10$\bar{1}$0) XRCs taken along the *c*-axis and *a*-axis, respectively.

second spatio-time-resolved cathodoluminescence (STRCL) technique to probe InGaAs/AlGaAs pyramidal nanostructures. As well as the scanning near-field optical microscopy, this technique is quite attractive in understanding diffusion and recombination processes of carriers and excitons in complex nanostructures, because of its high spatial and temporal resolutions. One of the advantages of using STRCL is that electron beam (*e*-beam) can excite carriers at the desired position of very high bandgap semiconductors. Using the same system, Corfdir *et al.*[18)] have investigated

*E-mail address: chichibulab@yahoo.co.jp

 © 2011 The Japan Society of Applied Physics

the relaxation and recombination dynamics of excitons bound to the I_1-type BSFs[19] in *a*-plane GaN epilayers grown using the lateral epitaxial overgrowth technique. However, local carrier dynamics in *m*-plane InGaN epilayers grown on the state-of-the-art *m*-plane FS-GaN has not been investigated yet.

In this article, the results of STRCL measurements on the very low TD and BSF density *m*-plane $In_{0.05}Ga_{0.95}N$ epilayer[15] grown on the high-quality FS-GaN substrate[10] are displayed. Local variation of the cathodoluminescence (CL) peak energy is attributed to a considerable difference in the local InN mole fraction caused by the residual structural imperfections. The bowing and tilt and twist mosaics of FS-GaN are shown to generate considerable overlayer structural imperfections, namely inclined and heavily tilted surface planes.

2. Experimental Procedure

A 70-nm-thick *m*-plane $In_{0.05}Ga_{0.95}N$ epilayer[15] was grown by MOVPE on a 325-µm-thick *m*-plane FS-GaN,[10] after growing an 1.5-µm-thick GaN underlayer.[20] The InGaN epilayer was confirmed by the X-ray reciprocal space mapping method to grow coherently[15] on the base GaN. As expected from the crystallographic orientation, so-called *V-defects* often observed in *c*-plane InGaN films[21] were absent. The FWHM values for the X-ray rocking curves (XRCs) of the InGaN epilayer were $\Delta\omega_{mc} = 163$ and $\Delta\omega_{ma} = 232$ arcsec for the $(10\bar{1}0)$ diffraction along the $\langle 0001\rangle$ and $\langle 11\bar{2}0\rangle$ azimuths, respectively, and $\Delta\omega_r = 43$ arcsec for the $(10\bar{1}2)$ diffraction. The result means that *m*-plane tilt mosaic, especially along the *a*-axis, is noticeable. These results are consistent with the fact that the *m*-plane FS-GaN substrate exhibted larger $\Delta\omega_{ma}$ value.[10,20] As shown in the plan-view and cross-sectional transmission electron microscopy (TEM) images in Figs. 2(a) and 2(b), respectively, distinct TDs or BSFs are not found in the $In_{0.05}Ga_{0.95}N$ layer.

Steady-state PL was excited using the 325.0 nm line of a cw He–Cd laser (125 W/cm^2). Spot-excitation (local) time-resolved CL measurement, namely STRCL measurement, was carried out using a picosecond pulsed electron gun equipped on a scanning electron microscope (SEM).[17,18] The pulsed *e*-beam was generated by irradiating the femtosecond pulses of a frequency-tripled mode-locked Al_2O_3:Ti laser (266 nm, 200 fs, 80.7 MHz) on the Au photocathode.[17] The acceleration voltage and probe current at the sample surface were 8 kV and 100 pA, respectively. The luminescence was dispersed by a grating monochromator and detected using a streak camera. The temporal resolution was approximately 10 ps. All the CL measurements were carried out at 32 K.

3. Results and Discussion

Macroscopic PL spectrum of the *m*-plane $In_{0.05}Ga_{0.95}N$ epilayer at 9 K exhibits a predominant NBE emission peak at 3.21 eV, as shown in the topmost trace in Fig. 3(a). It also exhibits a sharp peak at 3.458 eV and spectrally broad luminescence bands at around 2.8 and 2.2 eV. The latter three emissions are assigned, respectively, as being due to an unabsorbed bound excitonic emission, so-called blue luminescence band and yellow luminescence band originating from the GaN underlayer. The peak energy compared with that at 300 K and the FWHM value for the NBE

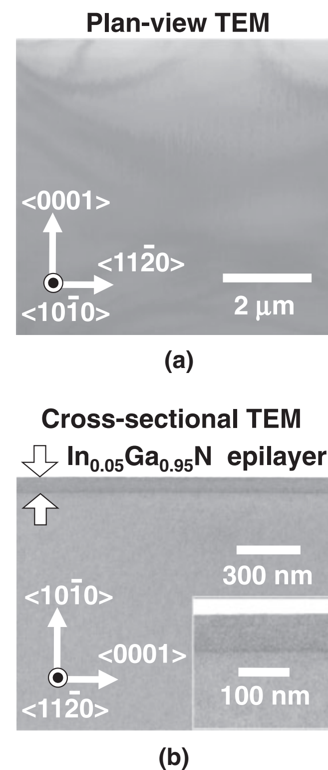

Fig. 2. (a) Plan-view and (b) cross-sectional TEM images for a 70-nm-thick *m*-plane $In_{0.05}Ga_{0.95}N$ epilayer grown on an *m*-plane FS-GaN. The *e*-beam incidence for (b) was parallel to the $\langle 11\bar{2}0\rangle$ axis.

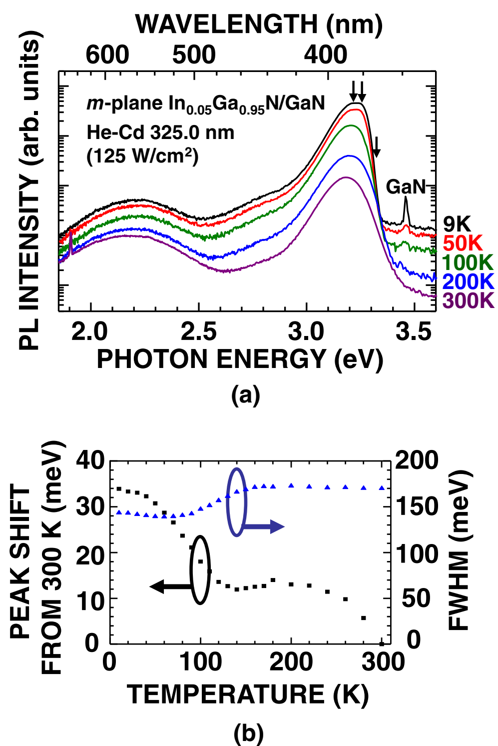

Fig. 3. (Color online) (a) Macroscopic PL spectra for the *m*-plane $In_{0.05}Ga_{0.95}N$ epilayer. Three vertical arrows indicate the energies at which the spatially-resolved CL intensity images in Figs. 4(b)–4(d) were taken. (b) The peak energy compared with that at 300 K and the FWHM value for the NBE emission peak of the $In_{0.05}Ga_{0.95}N$ epilayer plotted as a function of temperature.

© 2011 The Japan Society of Applied Physics

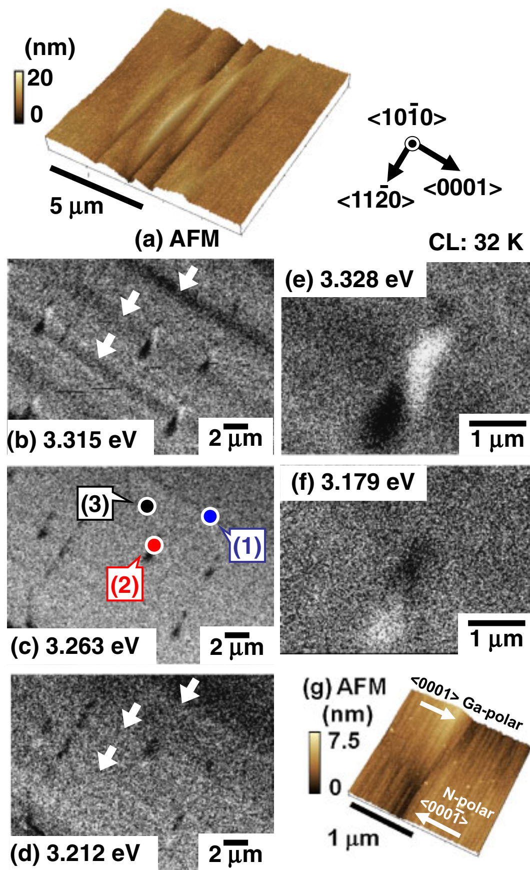

Fig. 4. (Color online) (a) The AFM image of the *m*-plane $In_{0.05}Ga_{0.95}N$ epilayer grown on the defective N-polar edge area of the wafer. Spatially-resolved monochromatic CL intensity images taken at (b) 3.315, (c) 3.263, and (d) 3.212 eV. Magnified CL intensity images taken around the figure-of-8 pattern at (e) 3.328 and (f) 3.179 eV. (g) Magnified AFM image for the area in the vicinity of the figure-of-8 pattern. All of the CL images were taken at 32 K with the 8 kV acceleration voltage. The markers (1)–(3) in (c) represent the positions where the STRCL signals shown in Fig. 5(b) were measured.

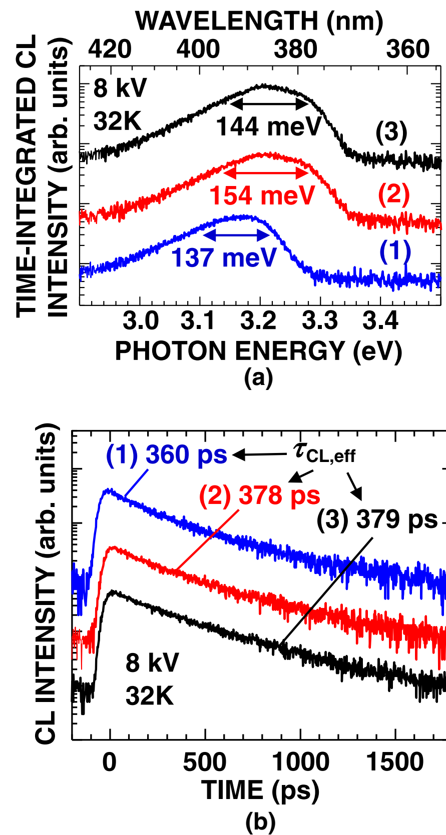

Fig. 5. (Color online) (a) Spot-excitation time-integrated CL spectra taken at the positions (1)–(3) in Fig. 4(c). (b) STRCL signals measured at the positions (1)–(3) in Fig. 4(c) at 32 K. The $\tau_{CL,eff}$ values are also shown.

emission peak are plotted as a function of temperature in Fig. 3(b). The PL peak energy first shifts to the lower energy by 21 meV between 40 and 150 K, followed by a considerable blueshift and the second moderate redshift with temperature rise. The gross shift being 34 meV is approximately a half of the bandgap energy change of GaN between 10 and 300 K (~65 meV).[22] The result implies the presence of certain bound-type band-tail states. The FWHM value for the NBE peak increases from 143 meV at 9 K to 170 meV at 180 K, indicating the thermal redistribution of excitons. Apparently, the FWHM values are larger than those for conventional *c*-plane $In_{0.05}Ga_{0.95}N$ film,[16] indicating that *m*-plane InGaN tends to have severer compositional inhomogeneity.

Although majority of the wafer exhibit flat surface morphology with monolayer or bilayer atomic step lines, approximately 5-µm-long inclined planes forming the striations along the *a*-axis (parallel to the *c*-plane) are often observed, as shown in the bird's-eye view atomic force microscopy (AFM) image in Fig. 4(a). Steady-state monochromatic CL intensity images taken at 3.315, 3.263, and 3.212 eV in the area close to Fig. 4(a) are shown in Figs. 4(b), 4(c), and 4(d), respectively. The monitored photon energies are shown by the arrows in Fig. 3(a). The image taken at 3.315 eV [Fig. 4(b)] exhibits striated dark zones (belts) almost parallel to the *c*-axis. However, the zonary pattern loses the contrast when the monitoring photon energy is lower than 3.263 eV, as shown in Figs. 4(c) and 4(d). Another distinct feature in Figs. 4(b)–4(d) is the presence of approximately 2-µm-long-axis, figure-of-8 patterns aligned parallel to the *a*-axis. The bright area within the figure-of-8 patterns is completely reversed in the monochromatic CL images taken at 3.328 and 3.179 eV, as shown in Figs. 4(e) and 4(f), respectively. Here we mention that the SEM image taken at the corresponding area is seen as featureless.

In order to explore the origin for the spatial and spectroscopic emission inhomogeneity shown above, STRCL spectroscopy was implemented. The time-integrated spot-excitation local CL spectra measured at 32 K for the positions marked by (1)–(3) in Fig. 4(c) are shown in Fig. 5(a). The monitored positions are within the (1) striated, dark CL-image zone at 3.315 eV, (2) higher CL peak energy area in the figure-of-8 pattern, and (3) featureless CL-image area. The peak energy and FWHM value for the CL peak in spot (1) are 3.17 eV and 137 meV, respectively. Because the NBE CL spectra for spots (2) and (3) contain higher energy emission components, the FWHM values of them are larger than that for (1). The result means that the bandgap inhomogeneity is severer in portions (2) and (3): i.e., they contain the areas of low InN mole fraction. Much severer compositional inhomogeneity has been found[12–14] in nonpolar $In_xGa_{1-x}N$ films grown on heteroepitaxial or defective sub-

 © 2011 The Japan Society of Applied Physics

strates. In those cases, the primary reason for the inhomogeneity is the presence of high density TDs and BSFs: they generate various inclined planes and facets having different surface bond configurations that have different In-incorporation efficiencies. Because the present m-plane $In_{0.05}Ga_{0.95}N$ film does not contain distinct TDs or BSFs, as shown in Fig. 2, the spectral inhomogeneity observed in Fig. 5(a) is probably due to considerable but non-negligible variation in the In-incorporation efficiency in the spots (1)–(3).

To verify this simple consideration, spectrally-integrated STRCL signals measured at the corresponding spots are shown in Fig. 5(b). As all the signals do not exhibit an ideal exponential decay shape, the effective CL lifetime ($\tau_{CL,eff}$) is defined[4] as the time after excitation when $\int_0^{\tau_{CL,eff}} I(t)\,dt / \int_0^{t_{lim}} I(t)\,dt$ becomes $1 - 1/e$, where $I(t)$ is the intensity at time t and t_{lim} is the time when $I(t_{lim})$ becomes $0.01I(0)$. The $\tau_{CL,eff}$ values are nearly constant irrespective to the position or photon energy: 360 ps for (1), 378 ps for (2), and 379 ps for (3). Here we note that the local CL spectra and local TRCL signal for the lower CL peak energy area within the figure-of-8 patterns are similar to those for the spot (1), indicating that InN mole fractions for both the areas are similar.

In a reasonable quality semiconductor, measured lifetime at 32 K is principally dominated by the radiative lifetime, because most of nonradiative processes are frozen. Then, the nearly identical and reasonably short $\tau_{CL,eff}$ value also excludes the possibility that BSFs limit $\tau_{CL,eff}$ values in the areas (1)–(3), because the radiative lifetime of excitons trapped in the I_1-type BSFs[19] or in the type-II quantum wells[23] formed within BSFs is much longer than the classical free or bound excitons in the case of GaN.[18] From the considerable CL peak energy variation being as small as up to 60 meV, as shown in Fig. 5(a), the InN mole fraction variation is estimated to be as small as $\pm 1\%$. This is the reason why remarkable change cannot be clearly found in the $\tau_{CL,eff}$ value in this study.

Because the morphological striation and m-plane tilt mosaic along the a-axis are severer than along the c-axis, the zonary pattern along the c-axis in the CL image [Fig. 4(b)] may not originate from the m-plane tilt mosaic along the a-axis. One of the possibilities for the higher and more homogeneous InN mole fraction in the zonary areas (1) is that the region may have $\langle 000\bar{1}\rangle$-oriented N-polar ($-c$) vicinal m-plane surface, due to the considerable tilt along the c-axis,[11] as In-incorporation efficiency for N-polar growth is higher than the Ga-polar growth according to the different atomic configurations.[24–26] The areas corresponding to spots (2) and (3) may contain flatter m-plane regions where In-incorporation efficiency is lower than that of other inclined vicinal planes.[14,15]

Finally, the reversed CL intensity image in the figure-of-8 patterns shown in Figs. 4(e) and 4(f) is attributed to the different In-incorporation efficiencies for different growth fronts. As shown in the AFM image in Figs. 4(a) and 4(g), the figure-of-8 patterns seem to exist at the positions where two vicinal planes inclined to opposite directions along the a-axis appear. Then, one of the growth fronts has an inclined Ga-polarity ($+c$) plane edge and the other has the N-polarity ($-c$) one. In this case, because In-incorporation efficiency for N-polar growth is higher than the Ga-polar growth, as described,[24–26] all the figure-of-8 patterns within the domain structure should have the same directional shapes. This is indeed the case, as confirmed by Figs. 4(b) and 4(d).

4. Conclusions

The STRCL spectroscopy was implemented for studying local carrier dynamics in the very low defect density, 70-nm-thick m-plane $In_{0.05}Ga_{0.95}N$ epilayer grown on an m-plane FS-GaN by MOVPE. In the spatially-resolved monochromatic CL intensity images, zonary patterns parallel to the c-axis and figure-of-8 reversal patterns aligned parallel to the a-axis were visualized. However, the low-temperature effective radiative lifetime quantified by STRCL did not show noticeable spatial variation. As TD or BSF was not found in the TEM images, the considerable CL peak energy variation is attributed to the local variation in the In-incorporation efficiency. For example, the appearance of opposite polarity ($+c$ and $-c$) growth fronts would generate the figure-of-8 patterns parallel to the a-axis, because the In-incorporation efficiency for the N-polar vicinal m-plane is higher than that for the Ga-polar and a-axis-inclined vicinal m-planes.

Acknowledgment

This work was supported in part by Grant-in-Aids of CANTech, IMRAM, Tohoku University and Scientific Research on Priority Areas (No. 18069001) from the Ministry of Education, Culture, Sports, Science and Technology, New Energy and Industrial Technology Development Organization programs by the Ministry of Economy, Trade and Industry, and Japan Student Services Organization, Japan. The work in Switzerland was supported by the National Centre of Competence in Research Quantum Photonics and Research Instrument of the Swiss National Science Foundation, Switzerland.

1) Review article, for example, see J. S. Speck and S. F. Chichibu: MRS Bull. **34** (2009) 304.
2) T. Takeuchi, S. Sota, M. Katsuragawa, M. Komori, H. Takeuchi, H. Amano, and I. Akasaki: Jpn. J. Appl. Phys. **36** (1997) L382.
3) S. Chichibu, T. Azuhata, T. Sota, and S. Nakamura: Appl. Phys. Lett. **69** (1996) 4188.
4) S. F. Chichibu, A. Uedono, T. Onuma, B. A. Haskell, A. Chakraborty, T. Koyama, P. T. Fini, S. Keller, S. P. DenBaars, J. S. Speck, U. K. Mishra, S. Nakamura, S. Yamaguchi, S. Kamiyama, H. Amano, I. Akasaki, J. Han, and T. Sota: Nat. Mater. **5** (2006) 810.
5) M. C. Schmidt, K.-C. Kim, H. Sato, N. Fellows, H. Masui, S. Nakamura, S. P. DenBaars, and J. S. Speck: Jpn. J. Appl. Phys. **46** (2007) L126.
6) K. Okamoto, H. Ohta, S. F. Chichibu, J. Ichihara, and H. Takasu: Jpn. J. Appl. Phys. **46** (2007) L187.
7) M. C. Schmidt, K.-C. Kim, R. M. Farrell, D. F. Feezell, D. A. Cohen, M. Saito, K. Fujito, J. S. Speck, S. P. DenBaars, and S. Nakamura: Jpn. J. Appl. Phys. **46** (2007) L190.
8) Y. Enya, Y. Yoshizumi, T. Kyono, K. Akita, M. Ueno, M. Adachi, T. Sumitomo, S. Tokuyama, T. Ikegami, K. Katayama, and T. Nakamura: Appl. Phys. Express **2** (2009) 082101.
9) A. Tyagi, R. Farrell, K. Kelchner, C. Huang, P. Hsu, D. Haeger, M. Hardy, C. Holder, K. Fujito, D. Cohen, H. Ohta, J. Speck, S. P. DenBaars, and S. Nakamura: Appl. Phys. Express **3** (2010) 011002.
10) K. Fujito, K. Kiyomi, T. Mochizuki, H. Oota, H. Namita, S. Nagao, and I. Fujimura: Phys. Status Solidi A **205** (2008) 1056.
11) A. Hirai, Z. Jia, M. C. Schmidt, R. M. Farrell, S. P. DenBaars, S. Nakamura, J. S. Speck, and K. Fujito: Appl. Phys. Lett. **91** (2007) 191906.
12) F. Bertram, S. Srinivasan, L. Geng, F. A. Ponce, T. Riemann, and J. Christen: Appl. Phys. Lett. **80** (2002) 3524.

© 2011 The Japan Society of Applied Physics

13) A. Chakraborty, S. Keller, C. Meier, B. A. Haskell, S. Keller, P. Waltereit, S. P. DenBaars, S. Nakamura, J. S. Speck, and U. K. Mishra: Appl. Phys. Lett. **86** (2005) 031901.
14) T. Koyama, T. Onuma, H. Masui, A. Chakraborty, B. A. Haskell, S. Keller, U. K. Mishra, J. S. Speck, S. Nakamura, S. P. DenBaars, T. Sota, and S. F. Chichibu: Appl. Phys. Lett. **89** (2006) 091906.
15) S. F. Chichibu, H. Yamaguchi, L. Zhao, M. Kubota, T. Onuma, K. Okamoto, and H. Ohta: Appl. Phys. Lett. **93** (2008) 151908.
16) S. Chichibu, T. Azuhata, T. Sota, and S. Nakamura: Appl. Phys. Lett. **70** (1997) 2822.
17) M. Merano, S. Sonderegger, A. Crottini, S. Collin, P. Renucci, E. Pelucchi, A. Malko, M. H. Baier, E. Kapon, B. Deveaud, and J. D. Ganière: Nature (London) **438** (2005) 479.
18) P. Corfdir, J. Ristić, P. Lefebvre, T. Zhu, D. Martin, A. Dussaigne, J. D. Ganière, N. Grandjean, and B. Deveaud-Plédran: Appl. Phys. Lett. **94** (2009) 201115.
19) C. Stampfl and C. G. Van de Walle: Phys. Rev. B **57** (1998) R15052.
20) S. F. Chichibu, H. Yamaguchi, L. Zhao, M. Kubota, K. Okamoto, and H. Ohta: Appl. Phys. Lett. **92** (2008) 091912 [Errata **93** (2008) 129901].
21) X. H. Wu, C. R. Elsass, A. Abare, M. Mack, S. Keller, P. M. Petroff, S. P. DenBaars, J. S. Speck, and S. J. Rosner: Appl. Phys. Lett. **72** (1998) 692.
22) S. F. Chichibu, T. Azuhata, T. Sota, and S. Nakamura: J. Appl. Phys. **79** (1996) 2784.
23) G. Salviati, M. Albrecht, C. Zanotti-Fregonara, N. Armani, M. Mayer, Y. Shreter, M. Guzzi, Y. V. Melnik, K. Vassilevski, V. A. Dmitriev, and H. P. Strunk: Phys. Status Solidi A **171** (1999) 325.
24) T. K. Zywietz, J. Neugebauer, and M. Scheffler: Appl. Phys. Lett. **74** (1999) 1695.
25) M. Sumiya, K. Yoshimura, K. Ohtsuka, and S. Fuke: Appl. Phys. Lett. **76** (2000) 2098.
26) T. Onuma, T. Koyama, A. Chakraborty, M. McLaurin, B. A. Haskell, P. T. Fini, S. Keller, S. P. DenBaars, J. S. Speck, S. Nakamura, U. K. Mishra, T. Sota, and S. F. Chichibu: J. Vac. Sci. Technol. B **25** (2007) 1524.

© 2011 The Japan Society of Applied Physics